

Risk Occupancy: A New and Efficient Paradigm through Vehicle-Road-Cloud Collaboration

Jiaxing Chen, Wei Zhong, Bolin Gao, Yifei Liu, Hengduo Zou, Jiaxi Liu, Yanbo Lu, Jin Huang, Zhihua Zhong

Abstract—This study introduces the 4D Risk Occupancy within a Vehicle-Road-Cloud architecture, integrating the road surface spatial, risk, and temporal dimensions, and endowing the algorithm with beyond-line-of-sight, all-angles, and efficient abilities. The algorithm simplifies risk modeling by focusing on directly observable information and key factors, drawing on the concept of Occupancy Grid Maps (OGM), and incorporating temporal prediction to effectively map current and future risk occupancy.

Compared to conventional driving risk fields and grid occupancy maps, this algorithm can map global risks more efficiently, simply, and reliably. It can integrate future risk information, adapting to dynamic traffic environments. The 4D Risk Occupancy also unifies the expression of BEV detection and lane line detection results, enhancing the intuitiveness and unity of environmental perception. Using DAIR-V2X data, this paper validates the 4D Risk Occupancy algorithm and develops a local path planning model based on it. Qualitative experiments under various road conditions demonstrate the practicality and robustness of this local path planning model. Quantitative analysis shows that the path planning based on risk occupation significantly improves trajectory planning performance, increasing safety redundancy by 12.5% and reducing average deceleration by 5.41% at an initial braking speed of 8 m/s, thereby improving safety and comfort. This work provides a new global perception method and local path planning method through Vehicle-Road-Cloud architecture, offering a new perceptual paradigm for achieving safer and more efficient autonomous driving.

Index Terms—ICV, 4D Risk Occupancy, OGM, Risk Field, Vehicle-Road-Cloud Collaboration Architecture, Local Path Planning.

I. INTRODUCTION

INTELLIGENT Connected Vehicle (ICV) is a key component of the Vehicle-Road-Cloud system. Compared to conventional autonomous driving, ICV can utilize roadside and cloud computing capabilities to obtain more comprehensive and accurate environmental information. Currently, there is no unified standard for perception and risk assessment in intelligent transportation and driving, but basic information such as the position and speed of objects is the main reference form. Refining these data into more advanced, cohesive perception forms enables intelligent vehicles to make more intuitive and interpretative decisions, serving as a vital supplement to conventional perception information.

This work was supported by Key Program of National Natural Science Foundation of China (52172389) and Hetao Shenzhen-HongKong Science and Technology Innovation Cooperation Zone (HZQB-KCZY-2021055). The authors are with the School of Vehicle and Mobility, Tsinghua University, Beijing 100084, China, and the State Key Laboratory of Intelligent Green Vehicle and Mobility, Tsinghua University, Beijing 100084, China. Jiaxi Liu is with the Civil and Environmental Engineering Department, University of Wisconsin-Madison, WI, 53715, USA. (e-mail: chenjx23@mails.tsinghua.edu.cn) (Corresponding author: Bolin Gao.).

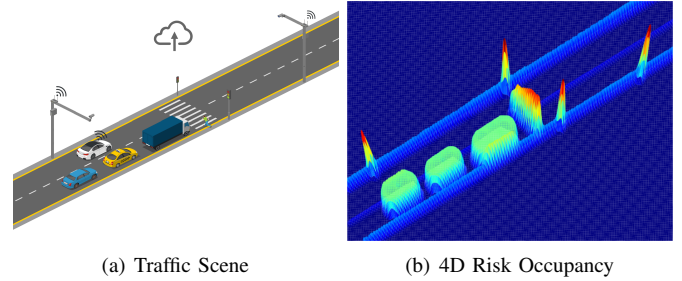


Fig. 1. When the green light comes on and a pedestrian runs across the road, the white ICV fails to recognize the runner due to the truck on the right front. Vehicle-Road-Cloud collaboration enables ICV to access the risk occupancy conditions for the next about 3 seconds, perceiving potential risks in advance.

At present, the intelligent driving industry extensively utilizes 3D object detection [1],[2],[3] or Bird's Eye View (BEV) object detection [4],[5] in conjunction with local map construction [6],[7],[8],[9]. The intermediate-layer features or result data produced are employed to support subsequent planning algorithms [10],[11],[12],[13]. In contrast to conventional perception paradigms, 4D risk occupancy perception paradigm can unify the above two, expressing lane lines and instance targets as corresponding risk occupancy situations and supporting subsequent planning tasks.

This study integrates the conventional driving risk field with the idea of OGM within the Vehicle-Road-Cloud collaborative architecture, offering a novel global perception approach essential for ICV operation in mixed traffic scenarios. In the field of driving risk field, it can be traced back to the work of Gerdes who proposed a driving assistance system based on the APF paradigm [14]. This method uses the field strength to construct an intuitive and unified driving environment, which can describe the inherent constraints of the road environment and collision risks. With the development of related theories, the construction method of the driving risk field model has become more complex, with more factors and methods participating in the risk field construction process. Wang's team established a driving risk field model composed of driver-vehicle-road factors [15],[16]. Many scholars continue to explore in the field of driving risk field research. For example, Han expanded the time dimension on the two-dimensional space, applying a three-dimensional spatiotemporal risk field to trajectory planning [17]. Tian et al. [18] improved the driving risk field for path planning and improved the A* algorithm [19] by adaptively expanding the direction and loss function. In addition, in the research [20], the impact of vehicle motion direction on driving risk and the relationship between potential

energy and force were considered, and the driving risk field model was improved, compared, and verified in the following car model. Wang et al. [21] constructed static and dynamic risk matrices for path planning and trajectory planning.

Cheng et al. [22] considered the issue of vehicle speed and acceleration, modifying the distance formula and kinetic energy field formula of the driving risk field, and [23] included vehicle acceleration and steering angle in the driving risk field model, all of which were finally applied to the vehicle following model. [24] proposed an extended driving risk field model, introducing vehicle geometric size, travel direction angle, and driving behavior characteristics, and using vehicle kinematics constraints for trajectory planning. Rasekhipour et al. [25] assigned different potential functions to different types of obstacles and road structures, and planned paths based on potential functions and vehicle dynamics. [26] quantified the risk of driving behavior, established a micro-risk field model, and proposed a trajectory and motion planning model on this basis. [27] built the multiple resolution of risk field by quadtree and realized the path planning for ego vehicle based on adaptive grid risk fields.

In conventional driving risk field, although many methods have been proposed, many modeling methods depend on parameters that are difficult to observe or quantify, such as road quality, adhesion coefficients, and vehicle parameters, which often need to rely on preset and subjective assignment. In addition, the diversity and complexity of driver behavior are influenced by many factors, such as personality, age, cultural quality, mood, state, etc. They are difficult to predict accurately. The increase in model complexity not only increases the pressure on computing resources and storage resources but also introduces a lot of uncertainty and noise, affecting the practical application and computational efficiency of the algorithm while reducing practicality and generality of model.

Occupancy grid mapping encapsulates information such as drivable areas and road obstacles, which is an important component of intelligent driving understanding of road scenarios. There have been many related studies over the years. For example, Wang and others [28] used particle filtering and multi-target tracking to achieve dynamic occupancy grid map construction, optimizing the accurate modeling of dynamic environments and target tracking. Zhao and others [29] optimized particle sampling, resampling, and map construction stages, and proposed an offline grid map resolution optimization scheme to improve map resolution while ensuring the real-time nature of the algorithm. Li [30] proposed a multi-vehicle collaborative local mapping method based on the fusion of occupancy grid maps, using genetic algorithms to optimize the objective function, and enhancing perception association ability through inter-vehicle relative posture estimation strategies. Toda [31] proposed a path planning algorithm based on multi-resolution occupancy grid maps, effectively reducing the consumption of computing resources in the process of finding feasible paths. The OGM algorithms for vehicle perception also include [32],[33],[34],[35],[36], etc. But the environmental perception methods based on OGM have not made a unified risk assessment of the driving environment.

To enhance computational efficiency and broaden the uni-

versality of algorithms, this study integrates driving risk assessment with the Occupancy Grid Map, proposing an innovative 4D Risk Occupancy algorithm. This algorithm builds upon the conventional two-dimensional road space model by introducing risk assessment and temporal dimension prediction, creating a four-dimensional model. This expansion effectively optimizes the model of the Occupancy Grid Map. By simplifying the complex parameters of vehicles, drivers, and roads in conventional risk field modeling and retaining only observable real-road information, the model complexity is reduced, enhancing its universality.

The overall algorithm of this study is based on the Vehicle-Road-Cloud collaborative framework, using directly observable perceptual data and unifying various factors of the road in the form of 4D risk occupancy to achieve an efficient assessment of road space risks. At the same time, this study has constructed a local path planning model based on 4D risk occupancy, aiming to improve the operational efficiency and practical application feasibility of the algorithm.

II. MODELING METHOD OF 4D RISK OCCUPANCY

In the field of ICV, following the conventional driving safety field, 4D Risk Occupancy has emerged as an innovative risk assessment method that plays a crucial role in the Vehicle-Road-Cloud perception architecture. This method unifies the multi-dimensional characteristics of potential risks in the road environment through quantification, providing effective support for ICV in subsequent key tasks such as planning and decision-making. This chapter will delve into the modeling techniques of 4D Risk Occupancy, covering key aspects such as risk quantification, sampling point and object interaction mechanisms, and the assessment process, aiming to provide a complete and concise theoretical framework.

A. Quantification Method of Road Risk

Road risk quantification is the foundation for constructing 4D Risk Occupancy. The first step in the quantification process is to identify and classify the risk factors that affect the driving safety of ICV. These risk factors are divided into two major categories: static factors and dynamic factors.

Static factors mainly cover fixed obstacles on the road, such as lane lines, guardrails, curbs, roadblocks, and potholes. Although these factors are relatively stationary in space, they may play a key role in the causation of traffic accidents. To quantify the risks of these static factors, this study assigns a fixed risk value and corresponding weight for each type of static obstacle. For instance, curbs and guardrails are given higher weights due to their significant constraints on vehicle travel paths. Potholes and lane lines are assigned lower weights due to their relatively minor impact on vehicle travel.

The quantification of static factors is essential for creating a comprehensive risk model that can be integrated into the path planning algorithms for ICV. By assigning appropriate risk values and weights, the model can better account for the potential hazards posed by various static elements within the driving environment, thereby enhancing the safety and reliability of ICV operations.

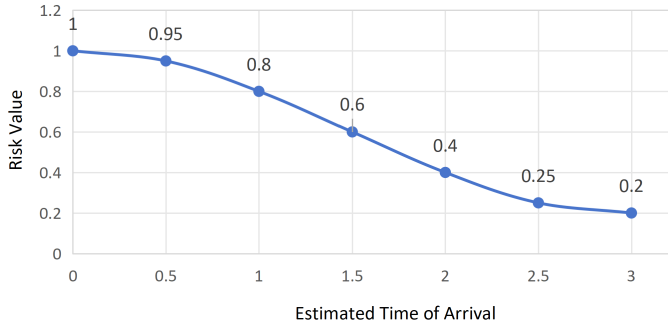


Fig. 2. The curvilinear relationship between risk value and ETA.

Dynamic factors such as human-driven vehicles, non-motor vehicles, and pedestrians, due to their ever-changing characteristics in time and space, pose a more direct and imminent threat to the driving safety of ICV. To quantify the risks associated with these dynamic factors, this study takes into account the critical information of traffic participants, such as their location, speed, and heading angle, and introduces the Estimated Time of Arrival (ETA) metric to quantify the level of risk these dynamic factors represent.

In the process of risk quantification, this study has established a principle that prioritizes personal safety and minimizes property damage as much as possible. Specifically, it gives the highest priority to avoiding direct collision injuries to individuals, meaning pedestrians and non-motorized vehicles are assigned the highest and second-highest risk weights, respectively. Next, it aims to avoid indirect injuries to individuals, with the risk weight for large vehicles being higher than that for small vehicles. This relationship indicates that an ICV colliding with a large vehicle would cause greater harm to the passengers on the ICV compared to a collision with a small vehicle. After that, the study considers dynamic factors to have a higher risk weight than static factors, meaning that colliding with and damaging other vehicles would result in greater property loss for both parties compared to static road infrastructure. By employing this weight distribution, it can assist ICV in prioritizing different risk scenarios, and in the event of an unavoidable situation, it tends to opt for a collision strategy with a lower risk.

2.5s is set as the safe time to meet the required time for most drivers to react and brake. For vehicles, under urban road scenarios with a speed limit of 70 km/h, autonomous braking generally requires less than 1.5 seconds. It can be assumed that once the ETA exceeds 1.5 seconds, the risk value will be significantly reduced, and as ETA increases, the magnitude of the risk value change will gradually diminish. Additionally, experimental results indicate that when a vehicle is stationary, assigning a risk value of 0.5 can reflect that stationary vehicles pose a higher risk compared to static factors, aligning with the principles of risk quantification.

The specific formulas are shown as in Eq. 1 and Eq. 2. Fig. 2 illustrates that this study has designed multiple points corresponding to different ETA values, and the relationship between ETA values and risk values obtained through non-linear regression is shown. The figure shows that the smaller

the ETA value, the higher the corresponding risk value, and exhibits a nonlinear negative correlation. At the same time, the risk value is normalized so that the risk value is in the range 0-1. This fully complies with the aforementioned trend and the principles of risk quantification followed by the study.

B. Sampling points and geometric object interaction method

To accurately assess road risks, dynamic and static factors are first converted into corresponding geometric objects, and a method based on the interaction between sampling points and geometric objects is designed. The placement strategy of sampling points and the interaction mechanism are crucial to ensuring the accuracy of risk assessment.

The arrangement of sampling points needs to take into account the width and direction of urban roads as well as the resolution of the road. This study adopts a uniform distribution strategy for placing sampling points on the road, as shown in Fig. 3, using a grid resolution of 1.9 meters to place sampling points. Each sampling point is responsible for assessing dynamic factors within a range of 2 meters and static factors within a range of 1 meter, thereby achieving an efficient evaluation of the risks in the road space. Traffic risk factors will be presented in the form of geometric objects, including single points, multiple points, line segments, and vectors. Single points are used to express the position of an object, multiple points are used to represent large area obstacles, line segments are used to indicate the object's position to the future, and vectors are used to express the layout direction and position of road solid lines, curbs, and guardrails.

During the interaction process, sampling points adopt a differentiated perception range radius strategy for static and dynamic objects. For static objects, a smaller perception range radius is set to reduce location errors and ensure a more precise risk occupancy position for static objects. For dynamic objects, the perception range radius is appropriately enlarged to capture more dynamic change information, thereby more effectively monitoring and predicting their risk occupancy situation. This flexible method of adjusting the perception range radius allows sampling points to adopt corresponding interaction strategies according to the dynamics of the object, ensuring both the precise identification of static objects and the sensitive capture of the behavior of dynamic objects.

For dynamic factors, [17] proposed that relying solely on the spatial dimension cannot fully express the complex changes of the dynamic traffic environment, and it is necessary to introduce the time dimension to represent risk in three-dimensional space-time. Future risk prediction for dynamic objects is very necessary, which helps ICV make reasonable and anticipatory local path planning decisions currently.

Different from the method of [17], in order to save computing resources and memory consumption, this study expresses three-dimensional space-time information on a two-dimensional plane. The 4D Risk Occupancy predicts the risk that will occur within the next 3 seconds for each dynamic object at the current moment. Out of a conservative strategy, the algorithm determines the position point that each traffic participant will reach after traveling at a constant speed and

$$ETA = \frac{Distance_{so}}{Speed}, \quad (1)$$

$$Risk_{dyn} = \begin{cases} 0.0667 \times ETA^3 - 0.3 \times ETA^2 + 0.0333 \times ETA + 1 & \text{if } ETA \leq 3.0 \\ 0.5 & \text{if } ETA > 3.0 \end{cases} \quad (2)$$

$$Risk_{sta} = \begin{cases} Constant & \text{if } Distance_{so} \leq 1.0 \\ 0 & \text{if } Distance_{so} > 1.0 \end{cases} \quad (3)$$

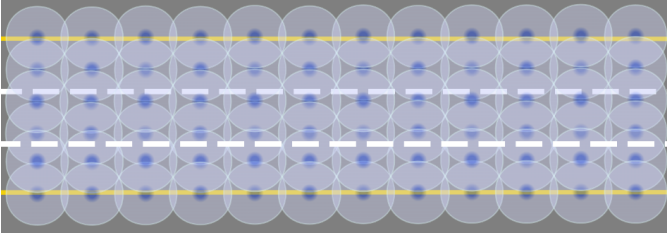


Fig. 3. Demonstration of the road sampling point layout. The sampling points on the road are arranged along the direction of the road with an adjustable resolution, and different sizes of resolution can be selected based on traffic flow density and computational resources.

direction for 3 seconds as its future position point and connects it to the current position coordinate point of the dynamic object to form a line segment. When these geometric objects enter the dynamic perception range of the sampling point, the ETA value between the sampling point and the position coordinate of the traffic participant is calculated, as shown in Eq. 1. Where $Distance_{so}$ is the distance from the sampling point to the dynamic object, and Speed is the speed of the dynamic object at that moment. This study uses polynomial fitting to obtain the Risk-ETA curve (as shown in Fig. 2 and Eq. 2), and uses this formula to calculate the potential collision risk value of each dynamic factor to the sampling point. For static factors, it is only necessary to detect whether the vectors and points enter the static perception range of the sampling point and assign a fixed risk value (0–1) and its weight according to the type of static factor, as shown in Eq. 3.

C. The Principle of 4D Risk Occupancy

The principle of 4D Risk Occupancy involves accumulating the risk values corresponding to multiple dynamic and static factors within the perceptual range of the sampling points to obtain the final road risk value. This process involves traversing the collection of sampling points and calculating the risk values. During the assessment process, this paper first defines the perceptual range of the sampling points and adopts corresponding interaction and calculation strategies based on the kind (static or dynamic) of the objects within that range. For dynamic objects, the ETA value needs to be calculated, and the potential collision risk is determined based on the ETA value. For static objects, a fixed risk value and weight are assigned directly according to the type of static object. The pseudo-code for the 4D Risk Occupancy calculation principle is shown in Algorithm 1.

Algorithm 1: Calculate Risk

Data: Coordinates of point, Data
Result: The calculated risk value

```

1 initialization;
2 for each dyn in dyns_info do
3     if distance ≤ 2.0 then
4         ETA ← dis_point_dyn / (speed_dyn + 0.01);
5         if ETA ≤ 3.0 then
6             degree_risk_dyn ← 0.0667 × ETA3 −
              0.3 × ETA2 + 0.0333 × ETA + 1;
7         else
8             degree_risk_dyn ← 0.5;
9         end
10        degree_risk ←
              degree_risk + degree_risk_dyn × weight_dyn;
11    end
12 end
13 for each stat in stats_info do
14     if distance < 1.0 then
15         degree_risk ←
              degree_risk + risk_value_stat × weight_stat;
16    end
17 end
18 return degree_risk;
    
```

After calculating the total risk value for each sampling point, this study aggregates and visualizes the risk values of all sampling points within the road area, presenting the intuitive and unified risk occupancy in road space from BEV, facilitating an intuitive understanding of the current and future driving risks in environment.

The risk occupancy results can not only represent the road occupancy but also distinguish the risks from various factors under different conditions. Fig. 4 illustrates the traffic situation at an intersection. The three cars driving straight on the upper right, due to their high speed, occupy a larger area and have a higher risk value; the car on the upper left slowing down for a red light has a smaller occupied area and a lower risk value; the stationary car waiting for the red light on the lower left has the smallest occupied area and the lowest risk value, indicating that stationary traffic participants pose less threat to ICV than those in motion. The figure also shows the risk occupancy of static factors such as the road median railing and curb, which are assessed to be lower in risk than dynamic

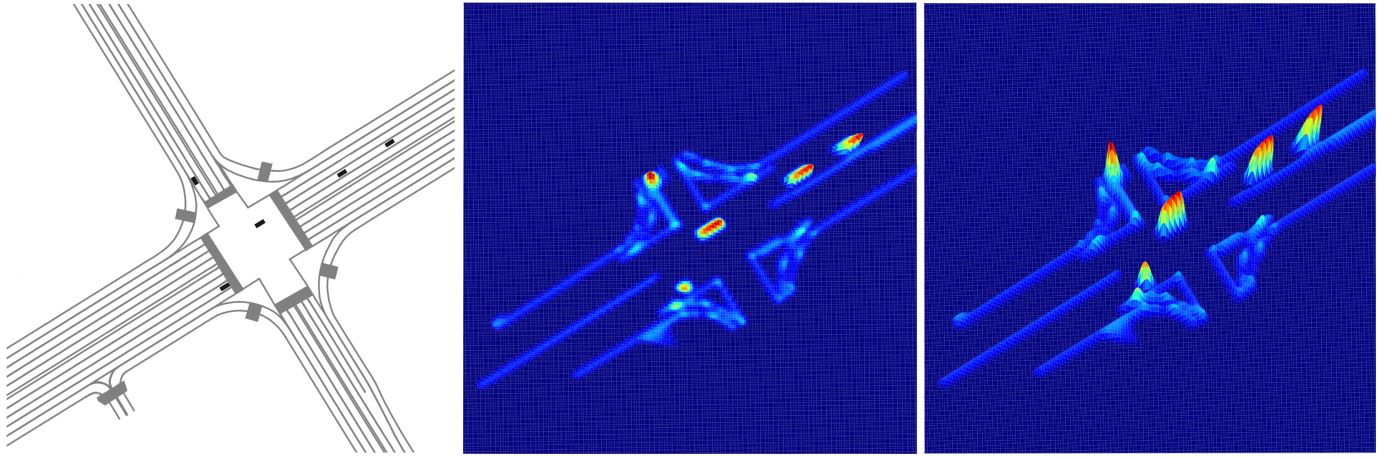


Fig. 4. Three images elucidate the 4D Risk Occupancy outcomes derived from the DAIR-V2X dataset. The image on the left depicts the perception result in BEV, providing an original perspective. The middle image presents the 4D Risk Occupancy map in BEV, offering an intuitive analysis of risk distribution. The image on the right transitions to a three-dimensional view, showcasing the 4D Risk Occupancy map in a format that enhances spatial understanding.

factors. All above is consistent with this study’s differentiation and evaluation of various factors and conditions.

III. A LOCAL PATH PLANNING APPROACH BASED ON 4D RISK OCCUPANCY

In this chapter, study designed an innovative local path planning method for ICV based on the characteristics of the 4D Risk Occupancy model. This method is intended to verify the applicability of 4D Risk Occupancy as an emerging perception method and its potential development value.

Based on the characteristics and advantages of the 4D Risk Occupancy and the Vehicle-Road-Cloud collaborative framework, this research has found that the path planning ideas of the A* algorithm series and the RRT algorithm series have potential applicability in combining risk occupancy fields. The A* algorithm is a heuristic search algorithm used to find the shortest path from the start point to the endpoint in a graph, guiding the search by evaluating the sum of the known cost of each node and the estimated remaining cost [19]. Tian et al. [20] integrated an elliptical formula into the driving risk field to address directional safety and obstacle avoidance, leading to a new A* path planning algorithm.

The RRT [37] and RRT* [38] algorithms, along with their variants, are sampling-based tree search methods suitable for complex, high-dimensional environments [39]. They efficiently explore feasible paths through random sampling and tree expansion, managing dynamic obstacles and constraints. A study [17] has expanded the temporal dimension by constructing a 3D STRF for trajectory planning. Wang and colleagues [40] have proposed a trajectory planning method for autonomous vehicles, combining potential fields with MPC, and developed a human-centered control strategy to balance safety, comfort, and smoothness in simulated environments.

The A* algorithm and its variants are suitable for path planning problems with clear start and end point, and they select paths by evaluating the sum of the known cost from the start point to the current point and the estimated cost from the current point to the end point. It is suitable for grid maps and can handle cost functions well. This type

of method is more suitable for the characteristics of the 4D Risk Occupancy algorithm under the Vehicle-Road-Cloud collaborative architecture.

A. Collision-free Dynamic Node Sets

Inspired by the pioneering work of the A* algorithm and its variants, this research has designed a local path planning algorithm driven by 4D Risk Occupancy within a Vehicle-Road-Cloud collaborative framework. On the edge cloud platform, future driving demands can be ascertained based on commands issued by the ICV. Subsequently, local path planning is conducted by leveraging the ICV’s current location, prior knowledge of lane information, and the assessment outcomes of the 4D Risk Occupancy model.

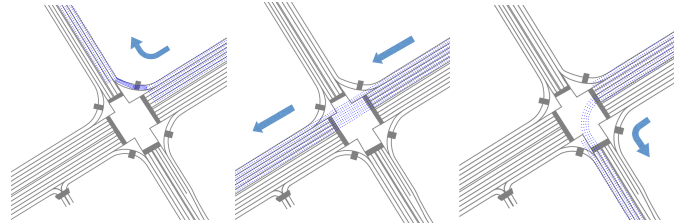


Fig. 5. The three figures show the cloud platform’s pre-set potential node sets for an ICV to navigate intersections, corresponding to three driving scenarios: right turn, straight, and left turn.

The algorithm initiates by preemptively retrieving a set of road points corresponding to the driving behavior instructions, based on the ICV’s current location, operational directives, and the road segment in which it is situated. The selection scope of this point set is predicated on the areas that can be potentially reached under the permissible conditions stipulated by traffic regulations. Fig. 5 illustrates the point sets for right turns, straight movements, and left turns that are stored on the edge cloud. When the ICV enters the intersection area, the edge cloud can extract the required preset point set based on the behavior instructions sent by the ICV. Subsequently, sampling points that fall below the preset risk threshold are repackaged into a collision-free dynamic node set. This collision-free

dynamic node set is updated with each frame to support dynamic planning.

B. Local Path Planning Strategy

The local path planning algorithm proposed in this study draws on the ideas of the A* heuristic search algorithm. It retrieves the positions of collision-free dynamic node sets and risks, and calculates the total cost of each path according to the heuristic function. The algorithm's path selection strategy is divided into two types: global optimization and local optimization. The global optimization strategy focuses on finding the path with the lowest comprehensive cost, but it takes a long time because it needs to calculate all paths. The local optimization strategy focuses on real-time performance, does not need to calculate all paths, and has a smaller overall computational load, although there is a risk of falling into a local optimum.

In consideration of computational efficiency, this study constructs a Frenet coordinate system based on the central line of the road for ICV to search for and select the next batch of path nodes. At the same time, a heuristic function is designed on the Cartesian coordinate system to guide the path search. Unlike the A* algorithm, this study uses the Euclidean distance from the nodes to the endpoint on the Cartesian coordinate system and the Euclidean distance from the starting point to the endpoint. At the same time, the road risk value is introduced into the cost calculation of the heuristic function. The node with the lowest heuristic function value in each row will be given the highest priority and added to the closed set. The heuristic function is as follows:

$$Score = weight_{risk} \times risk + weight_{dis} \times \frac{\sqrt{(x_{sample} - x_{dest})^2 + (y_{sample} - y_{dest})^2}}{\sqrt{(x_{icv} - x_{dest})^2 + (y_{icv} - y_{dest})^2}}, \quad (4)$$

where (x_{sample}, y_{sample}) , (x_{icv}, y_{icv}) and (x_{dest}, y_{dest}) respectively are the position coordinate of the sample point, ICV, and destination point. The weights of risk cost and distance cost can be set according to the effect.

The global optimization strategy first determines a preset endpoint based on future driving actions and obtains the collision-free dynamic node set at the current moment. It determines all possible road nodes that can be reached according to the position and direction of the ICV, calculates the cost of all batches of neighboring nodes, and finally selects a path with the lowest total cost value, such as a series of algorithms based on RRT. Unlike the global optimization strategy, the local optimization strategy does not need to calculate all possible road nodes that can be reached. It only needs to select the node with the smallest cost value in each batch of neighboring nodes, as shown in the node of the optimum path module in Fig. 6. The node set of the optimal path shows that the red nodes signify nodes of high risk, and the yellow nodes represent the locally optimal path nodes obtained by a strategic selection. The blue ones indicate the low-risk candidate nodes. The dashed frames denote the search domain for each batch.

The algorithm starts at a given node (the position of ICV) and identifies the next set of adjacent nodes based on the direction of travel according to predefined rules. It then repeatedly applies the same method to these adjacent nodes. This process continues until one of the following two conditions is met: either the algorithm reaches the target endpoint or it exhausts all feasible nodes without reaching the endpoint. At this point, the search ends, and the algorithm returns the best path found.

For this purpose, this paper designs a rule to determine the next batch of neighboring nodes. Based on the prior knowledge of the road space location, each row of the node set is numbered in advance. Then, based on the future behavior of the ICV and traffic regulations, the movement rules are determined. The advantage of this is that it can reduce the search range of the next batch of nodes and greatly reduce the amount of calculation. For example, when the ICV needs to turn left at the intersection in the future, as shown by the blue dashed frame in the node of the optimum path module in Fig. 6, the nodes of each batch can only select the nodes in the straight direction and the nodes two to the left in the next row of nodes, guiding the ICV to move to the left as early as possible before entering the intersection and prepare to enter the farthest left lane to complete the left turn.

The local path planning algorithm constructed based on the 4D Risk Occupancy model typically generates an initial trajectory composed of a series of short line segments, forming a rough path. These trajectories, connected by short line segments, may not be smooth enough for practical application, affecting the vehicle's driving comfort and efficiency. To address this issue, this study employs Gaussian trajectory smoothing techniques to further optimize the generated trajectory. Specifically, the algorithm first applies Gaussian filtering to each node in the original trajectory, creating a new set of smoothed trajectory nodes by weighted averaging of trajectory nodes based on the predetermined Gaussian kernel size and standard deviation. Then, the algorithm further refines these smoothed nodes through interpolation techniques, such as spline interpolation or polynomial interpolation, to generate a smoother and more continuous trajectory. With Gaussian trajectory smoothing processing, the trajectory generated by the algorithm is not only smoother but also more practical, enhancing the comfort of vehicle travel while maintaining the advantages of the original path planning.

IV. DESIGN OF VEHICLE-ROAD-CLOUD COLLABORATION ARCHITECTURE

This chapter will introduce the research process and the application architecture of Vehicle-Road-Cloud (VRC) collaboration. Within the framework of VRC collaboration, this study has implemented an assessment of road risk occupancy and a local path planning algorithm. The goal is to make full use of the synergistic effects and advantages of vehicles, road infrastructure, and cloud computing resources to provide ICV with more comprehensive and efficient services.

A. The Pipeline of Algorithms

This study presents an integrated framework for road risk occupancy assessment and local path planning algorithms, as

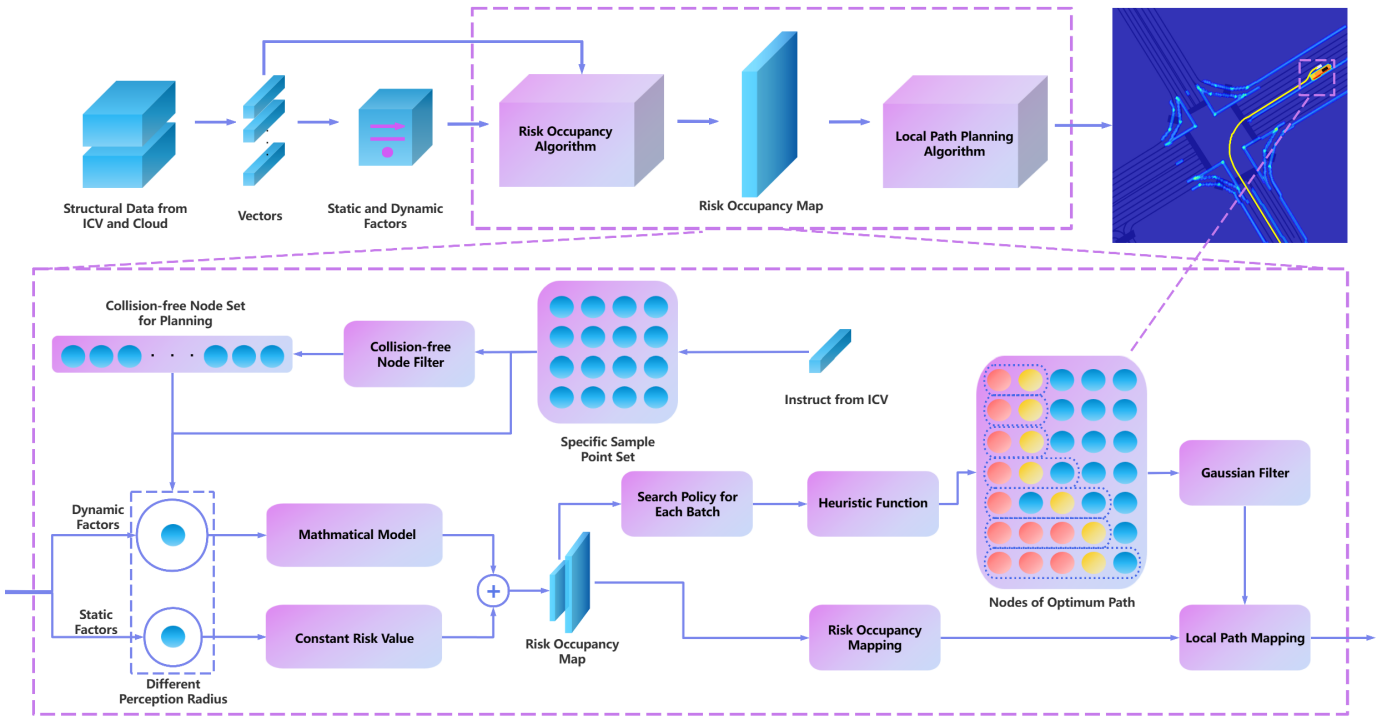


Fig. 6. The Structural Principle of the 4D Risk Occupancy Algorithm and Local Path Planning Algorithm.

shown in Fig. 6. The operational process of this framework is as follows: Initially, data collected from ICV, roadside perception units, and edge cloud storage are integrated and split into independent data vectors, which are then further transformed into corresponding geometric objects for subsequent processing. When the edge cloud platform receives instructions uploaded by the ICV, the system will retrieve the pre-stored specific road surface point sets based on the future action requirements (left turn, go straight, or right turn) indicated in the instructions. The system filters out road sampling points with risk values below a preset threshold; these points are considered collision-free nodes and are stored sequentially. For different types of factors (dynamic or static), each sampling point adopts a perception range of different sizes. As shown in Fig. 6, for dynamic factors, the perception range of the sampling points is larger because their positions change constantly over time, posing a greater threat to safety. Accordingly, the tolerance for position errors for dynamic factors is higher, and the algorithm can expand the occupancy prediction range of the sampling points to enhance the driving safety redundancy of ICV on the road. Conversely, static factors require more precise location descriptions, so the perception range of the sampling points is smaller to avoid misjudging the risk occupancy situation.

The system adopts different distance calculation methods for different types of factors and different geometric objects (points, line segments, and vectors). The interaction between dynamic factors and sampling points is calculated through mathematical models to determine risk, while static factors are directly assigned fixed risk values based on the type of obstacle. These dynamic and static risk values are then

accumulated to determine the total risk value of each sampling point. As shown in Fig. 6, the algorithm traverses all road sampling points in the specific point set and the collision-free node set and calculates the road risk occupancy according to the above method, generating a 4D Risk Occupancy map. The 4D Risk Occupancy map generated by the specific point set covers a larger intersection area, showing the risk occupancy over a wider area. The 4D Risk Occupancy map generated by the collision-free node set, on the other hand, selects the optimal nodes on the road ahead of the ICV through the locally optimal path search strategy designed in this study, combined with heuristic functions. Finally, the calculated road risk occupancy map is combined with the local path to show the mapping result.

B. Vehicle-Road-Cloud Collaboration Application Architecture

This paper presents a 4D Risk Occupancy algorithm and a local path planning algorithm designed to operate on the edge cloud within a Vehicle-Road-Cloud collaborative framework. These algorithms on the cloud platform are engineered to receive diverse data from ICV, roadside infrastructure, and cloud services, focusing on serving ICV by providing real-time risk occupancy assessment and local path planning for their respective road regions. The system initially constructs a structured dataset inclusive of static elements using prior information and integrates dynamic data collected by roadside perception devices, such as the type, location, velocity, and heading angle of traffic participants. This data is transmitted to the edge cloud server, where it undergoes a coordinate transformation from the geodetic coordinate system to the

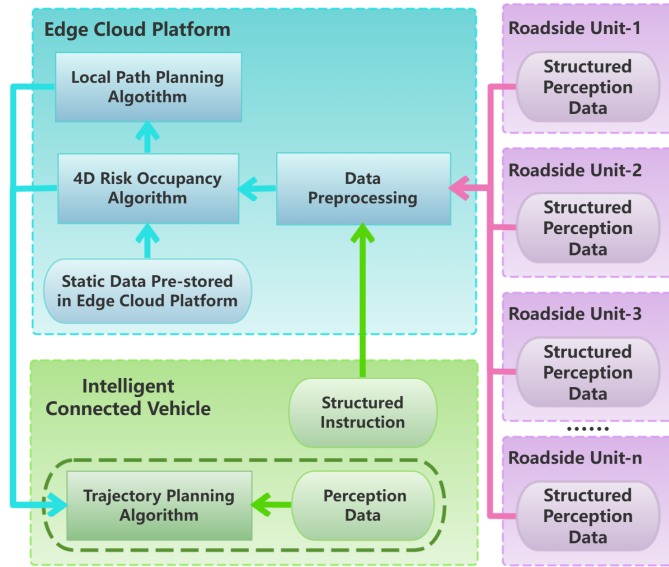


Fig. 7. Flowchart of 4D Risk Occupancy algorithm and its local path planning algorithm under Vehicle-Road-Cloud Collaboration architecture.

Cartesian coordinate system, and the ICV’s location is identified based on the instructions uploaded by the ICV. The algorithms selectively display the risk occupancy of local road areas to enhance computational efficiency and complete local path planning based on road risk occupancy, transmitting the planning results and risk occupancy information back to the ICV to support its decision-making.

As illustrated in Fig. 7, the content within the dashed frame at the vehicle end is not part of the algorithm development of this paper; it is merely for explanatory purposes. The output of our algorithm can potentially serve as input for subsequent vehicle-end algorithms, enabling a wider array of applications. Although the subsequent algorithms may utilize the results of our system, their development and implementation are not within the scope of this study. The presentation of these potential application scenarios in this paper is intended to highlight the multifunctionality and expandability of the algorithm’s output. However, the detailed implementation of the specific algorithms will be addressed in future research.

In addition, The purple section on the right side of Fig. 7 represents multiple roadside perception units, demonstrating the advantages of the algorithm in the cloud, which is to obtain perception information from multiple roadside units, achieving beyond-line-of-sight and global information perception that cannot be achieved by a single vehicle end.

Within the Vehicle-Road-Cloud collaborative framework, the design of the perception algorithm seamlessly integrates a priori information from the cloud with dynamic data from vehicle and roadside sources. This integrated approach not only enhances the flexibility of data processing but also significantly reduces reliance on computational power and memory resources. This optimized data processing strategy allows the algorithm to operate more efficiently while maintaining low resource consumption. Furthermore, the framework, through multi-node roadside perception devices, provides the algorithm with a comprehensive perspective, achieving beyond-line-of-

sight and panoramic road information collection. This all-encompassing perception capability greatly enhances the algorithm’s understanding and predictive abilities regarding traffic conditions, enabling it to assess and respond to various traffic scenarios more accurately. Additionally, the high-performance servers of the edge cloud platform provide robust support for the perception algorithm. The combination of low latency and high computational power allows the algorithm to quickly process vast amounts of data, thus achieving real-time decision-making and response. This rapid data processing capability is crucial for autonomous vehicles, as it directly affects their adaptability and safety in complex traffic environments.

In summary, the perception algorithm under the Vehicle-Road-Cloud collaborative framework, through the integration of cloud information with vehicle and roadside data, comprehensive monitoring by multi-node perception devices, and the high-performance computing of the edge cloud platform, together constructs an efficient, flexible, and responsive intelligent transportation system. This not only provides strong decision support for ICV but also lays a solid foundation for the development of future intelligent transportation.

V. ANALYSIS OF EXPERIMENTAL RESULTS

The 4D Risk Occupancy algorithm was validated using the DAIR-V2X dataset [41]. As shown in Fig. 8, the algorithm’s feasibility and applicability were tested in an intersection scenario, where the target ICV is represented by a white rectangle and the HDV by a black rectangle. Road risk values are depicted using a gradient from dark blue to dark red, indicating increasing risk levels.

The study further qualitatively analyzes the effectiveness of the local path planning algorithm within a Vehicle-Road-Cloud collaborative framework through three designed scenarios for the ICV entering the intersection: right-turn, straight-forward, and left-turn, with yellow lines indicating the planned path. Four sequential frames of 4D Risk Occupancy visualization were extracted to show the algorithm’s effectiveness under various traffic conditions. Furthermore, to quantitatively assess the advantages of 4D Risk Occupancy-based path planning, a comparative analysis was conducted with a trajectory planning algorithm that accepts path guidance. This comparison aimed to evaluate the impact of using 4D risk occupancy and local path planning information versus not using them.

A. Qualitative Experiment

1) *ICV Right-Turn Behavior Experimental Analysis:* To validate the effectiveness of the local path planning algorithm based on the 4D Risk Occupancy model when an ICV approaches an intersection and prepares to execute a right-turn maneuver, study designed two representative test scenarios. These scenarios simulate the driving states of the ICV at different times and positions.

Firstly, the first row of images in Fig. 8 sequentially displays four steps of the first right-turn scenario. In this scenario, the ICV is traveling straight in the third lane from the right and preparing to make a right turn. A HDV overtakes the ICV from behind in the far right lane at a faster speed and enters

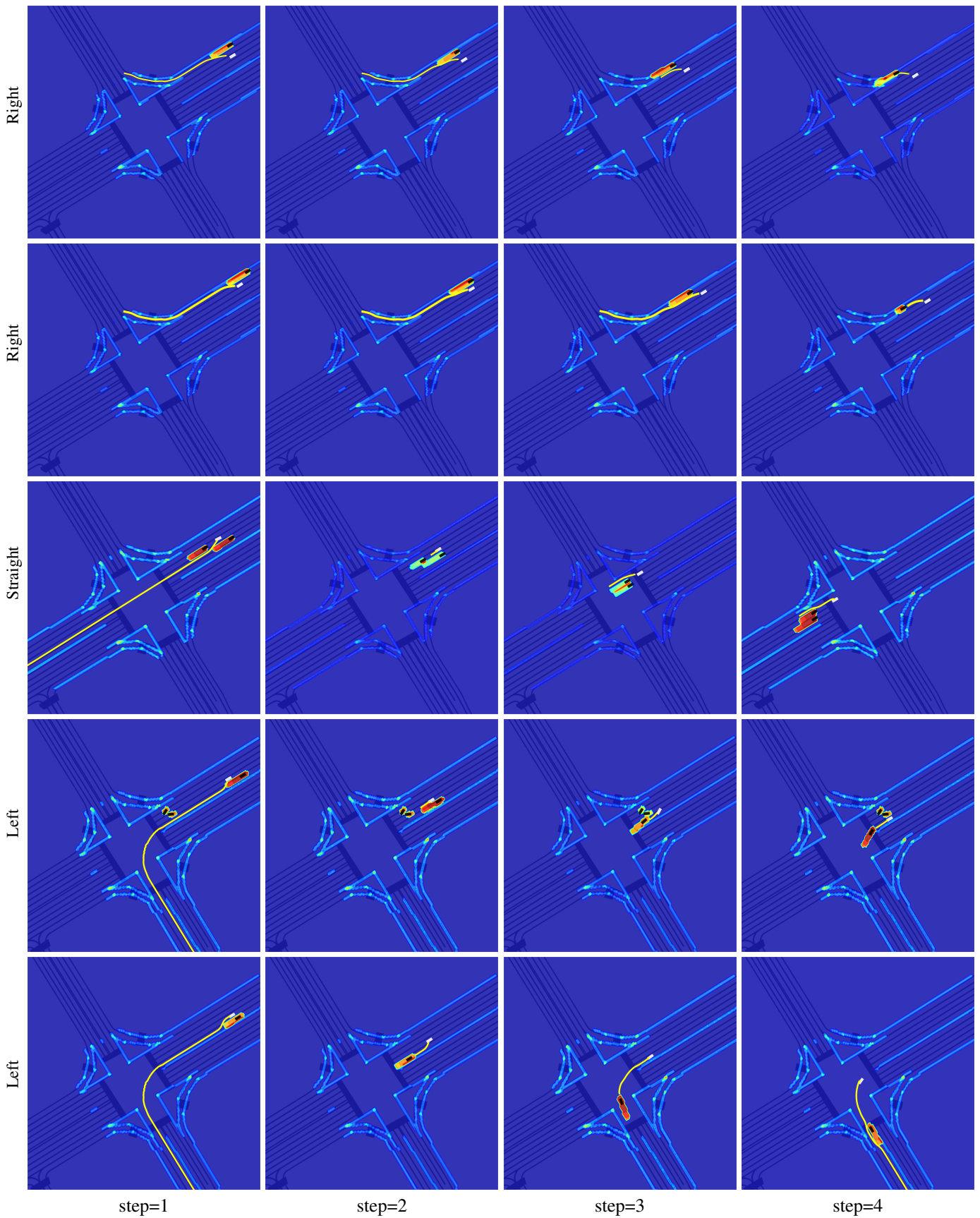


Fig. 8. Performance of local path planning algorithm based on 4D Risk Occupancy under various conditions when entering intersections.

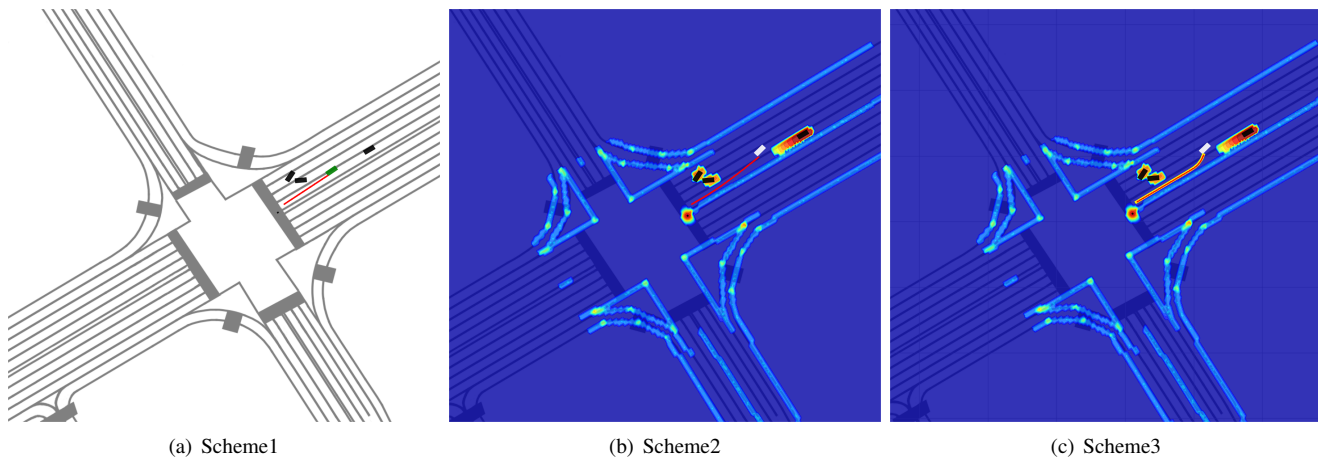


Fig. 9. The trajectory planning outcomes, as identified by ICV when detecting pedestrians, are presented under three distinct quantization experimental schemes. The trajectory planning results are delineated by a sequence of red points.

TABLE I
COMPARISON OF THREE DIFFERENT SCENES SCHEMES

Scheme	Trajectory Planning	4D-Risk-Occ	Path Planning	Max Safety Speed	Average Acceleration	Behavior Pattern
1	✓	-	-	5.42 m/s	-0.634 m/s ²	Dangerous
2	✓	✓	-	8.875 m/s	-0.536 m/s ²	Normal
3	✓	✓	✓	9.00 m/s	-0.507 m/s ²	Obey Rules

the right-turn ramp first. From the images in step 1 to step 3, it can be observed that as the ICV is overtaken by the HDV on the right, its path planning for lane change to the right is influenced by the risk occupancy in front of the HDV. The path planning algorithm adjusts its strategy accordingly, initially guiding the ICV to change lanes to the right, adjacent to the lane where the HDV is located. Then, it guides the ICV to drive straight over the risk area of the HDV and change lanes to the right again, smoothly entering the single-lane right-turn ramp. In the image of step 4, it can be seen that when the risk occupancy of the HDV connects with the solid-line risk occupancy of the right-turn single lane, the path planning algorithm tends to adopt a more cautious strategy. At this point, the algorithm guides the ICV to first change to the adjacent lane and continue straight, waiting for the HDV and ICV to have sufficient distance in terms of road travel direction before changing lanes to the right and following the HDV into the right-turn ramp.

The second row of images presents the second typical scenario encountered by the ICV when executing a right-turn maneuver. In this scenario, the ICV is traveling straight in the second lane from the right and needs to change lanes to the right in advance to complete the right turn at the intersection. However, an HDV overtakes the ICV from behind in the far right lane until it enters the right-turn ramp first. In step 1, the local path planning algorithm recommends that the ICV change lanes directly based on the current traffic situation. But in steps 2 and 3, as the HDV overtakes from the right rear at a faster speed, the path planner adjusts its strategy, choosing to first drive straight over the risk occupancy in front of the HDV and then change lanes to the right, rather than changing lanes

immediately, to ensure the safety of the ICV's lane change.

In step 4, the HDV begins to slow down in preparation for entering the right-turn ramp, and the risk occupancy area in front of the HDV decreases. At this time, the ICV and HDV have created a certain distance in terms of the direction of travel, and the path planner recommends immediately changing lanes to the right to follow the HDV into the right-turn ramp. It can be seen that the local path planning algorithm based on 4D Risk Occupancy is effective and applicable in ensuring the driving safety of the ICV.

2) *ICV Straight-Forward Behavior Experimental Analysis:* The third row in Fig. 8 demonstrates the scenario of an ICV proceeding straight through an intersection. In this scenario, before the ICV enters the intersection, there are HDVs traveling straight ahead and to the left rear, close by, and as time progresses, the relative positions of these three vehicles change. These four steps illustrate the adaptability and applicability of the local path planning algorithm in response to complex and dynamic straight-forward driving conditions.

Specifically, in the third row's step 1, it can be observed that before the road space risk occupancy of the two HDVs is about to enclose, the path planning recommends that the ICV change lanes to the upper left to overtake. This strategy aims to utilize the available road space to avoid being restricted by the HDVs on both sides.

In step 2, when the road risk occupancy of the two HDVs occupies the road in front and to the upper left of the ICV, the ICV adopts a conservative strategy and chooses to follow in a straight line. In steps 3 and 4 after entering the intersection, the path planning recommends overtaking the HDVs ahead from the right and conservatively suggests overtaking and

then proceeding straight after changing to the right lane. Compared to bypassing the two HDVs from the left, this strategy is obviously less costly because it takes advantage of the potentially lower traffic flow on the right and reduces the number of lane changes and potential conflict points.

3) *ICV Left-Turn Behavior Experimental Analysis:* From the fourth row of images in Fig. 8, it can be observed that when the ICV is preparing to enter the intersection and execute a left-turn maneuver, it faces the risk occupancy brought by a HDV from the left rear, and the path planner adopts a wise strategy. In step 1, the path planner recommends that the ICV first change lanes to the upper left avoid the risk occupancy area of the HDV from the left rear and complete the left lane change to overtake. Subsequently, the ICV will proceed straight into the intersection and execute the left turn.

In steps 2 and 3, the situation changes: the HDV from the left rear overtakes the ICV at a faster speed. Faced with this new situation, the path planner recommends that the ICV adopt a conservative but safe strategy: first change lanes to the left, then follow the HDV in a straight line, and follow the HDV to make a left turn at the appropriate time, rather than taking a risky strategy, and try to overtake the HDV on the outside and then make a left turn. This strategy reflects the path planning fully considers traffic rules and driving safety in strategy selection, avoiding potential conflicts and risks.

Through the above scenario simulation, it is demonstrated that the path planning algorithm based on 4D Risk Occupancy can dynamically adjust the planning strategy according to real-time traffic conditions and the behavior of surrounding vehicles, ensuring the safety and compliance of driving.

B. Quantitative Experiment

The experimental scenario is an ICV left-turn scenario, where there is a collision between two vehicles in front of the ICV, blocking the road. Meanwhile, there is a vehicle moving forward behind the ICV on the left, and pedestrians are crossing the road against the traffic light, as shown in Fig. 1. In this study, a trajectory planning algorithm[42] capable of tracking the target path is utilized to quantify the impact of the risk occupancy algorithm and its local path planning algorithm on the driving safety of ICV. Considering the balance of safety and comfort, the maximum deceleration for braking the ICV is set to -4.0 m/s^2 .

Table I and Fig. 9 show the differences among the three schemes: In scheme 1, neither the risk occupancy nor the path planning algorithm are used. Since the ICV detects the pedestrian relatively late, the available braking distance is shorter, and its maximum initial safety speed redundancy is 5.42 m/s . Based on its maximum safe redundancy speed of 5.43 m/s , the average acceleration of the ICV at this time is -0.634 m/s^2 .

In scheme 2, the risk occupancy is used. The ICV detects the pedestrian earlier than in scheme 1 through the risk occupancy of the pedestrian and begins to decelerate at this time. The maximum safety speed redundancy at this time is 8.875 m/s . To compare with the subsequent scheme 3, an initial braking speed of 8.0 m/s is used as the calculation premise, so its average braking acceleration is -0.536 m/s^2 .

The trajectory planning performs normally, but the lane change completion time is too long. In scheme 3, both risk occupancy and path planning are enabled. Compared with scheme 2, the maximum safety speed redundancy slightly increases to 9.0 m/s . When the initial braking speed is 8 m/s , its average braking acceleration is -0.507 m/s^2 , which is smaller than scheme 2, resulting in better comfort. At the same time, the trajectory planning algorithm with path planning guidance results in a shorter lane change completion time, demonstrating a high level of compliance with traffic regulations. This ensures safe and rule-abiding driving behavior.

Through quantitative experimental analysis and guidance of path planning based on risk occupation, the performance of trajectory planning tasks has significantly improved compared to tasks without path planning guidance. With the premise of ensuring pedestrian safety, the maximum safe braking initial speed redundancy has increased by 12.5%, and at a braking initial speed of 8.0 m/s , the average deceleration during the braking process has decreased by 5.41%, leading to improvements in both safety and comfort.

VI. CONCLUSION

This study introduces an innovative 4D Risk Occupancy algorithm in response to the safety driving requirements of intelligent connected vehicles under a Vehicle-Road-Cloud collaborative architecture. The algorithm optimizes conventional driving risk field modeling by unifying directly observable perceptual data into a 4D risk occupancy form, thereby efficiently assessing the risk within road space. Additionally, a local path planning model based on 4D risk occupancy was constructed, demonstrating the robustness of the path planning algorithm across various driving conditions, with the aim of verifying the effectiveness and applicability of high-level perceptual forms such as 4D risk occupancy. Furthermore, the designed Vehicle-Road-Cloud collaborative application architecture ensures that the algorithm can receive and process data from vehicles, roadside perception units, and edge clouds in real time, offering ICV a more comprehensive and unified risk assessment method in complex mixed traffic scenarios, thereby enriching the theoretical research methods of risk perception in Vehicle-Road-Cloud collaborative systems.

Despite demonstrating potential in perception and planning within the Vehicle-Road-Cloud collaborative architecture, the study has certain limitations. Firstly, the 4D Risk Occupancy algorithm is not an end-to-end perceptual solution but relies on upstream BEV perception results. This makes the accuracy and reliability of the algorithm susceptible to errors or noise from upstream modules and puts some pressure on perceptual timeliness. Secondly, to achieve efficient operation of the algorithm, detailed mapping of roads by the cloud platform is required to obtain prior information. This requirement may increase implementation costs and limit the algorithm's universality and flexibility in different road environments.

Future studies may delve into the enhancement and refinement of an end-to-end 4D risk occupancy assessment model. This progression could pave the way for the inception of more advanced and robust trajectory planning algorithms within the Vehicle-Road-Cloud collaborative framework.

REFERENCES

- [1] Junbo Yin, Jianbing Shen, Runnan Chen, Wei Li, Ruigang Yang, Pascal Frossard, and Wenguan Wang. Is-fusion: Instance-scene collaborative fusion for multimodal 3d object detection, 2024.
- [2] Chunyong Hu, Hang Zheng, Kun Li, Jianyun Xu, Weibo Mao, Maochun Luo, Lingxuan Wang, Mingxia Chen, Qihao Peng, Kaixuan Liu, Yiru Zhao, Peihan Hao, Minzhe Liu, and Kaicheng Yu. Fusionformer: A multi-sensory fusion in bird's-eye-view and temporal consistent transformer for 3d object detection, 2023.
- [3] Kai Lei, Zhan Chen, Shuman Jia, and Xiaoteng Zhang. Hvdetfusion: A simple and robust camera-radar fusion framework, 2023.
- [4] Haotian Hu, Fanyi Wang, Jingwen Su, Yaonong Wang, Laifeng Hu, Weiye Fang, Jingwei Xu, and Zhiwang Zhang. Ea-iss: Edge-aware lift-splat-shot framework for 3d bev object detection, 2023.
- [5] Hongxiang Cai, Zeyuan Zhang, Zhenyu Zhou, Ziyin Li, Wenbo Ding, and Jiahua Zhao. Bevfusion4d: Learning lidar-camera fusion under bird's-eye-view via cross-modality guidance and temporal aggregation, 2023.
- [6] Ruihao Wang, Jian Qin, Kaiying Li, Yaochen Li, Dong Cao, and Jintao Xu. Bev-lanedet: a simple and effective 3d lane detection baseline, 2023.
- [7] Hang Wu, Zhenghao Zhang, Siyuan Lin, Tong Qin, Jin Pan, Qiang Zhao, Chunjing Xu, and Ming Yang. Blos-bev: Navigation map enhanced lane segmentation network, beyond line of sight, 2024.
- [8] Tianyuan Yuan, Yicheng Liu, Yue Wang, Yilun Wang, and Hang Zhao. Streammapnet: Streaming mapping network for vectorized online hd map construction, 2023.
- [9] Zewen Zheng, Xuemin Zhang, Yongqiang Mou, Xiang Gao, Chengxin Li, Guoheng Huang, Chi-Man Pun, and Xiao Chen. Pvalane: Prior-guided 3d lane detection with view-agnostic feature alignment. In *AAAI Conference on Artificial Intelligence*, 2024.
- [10] Diankun Zhang, Guoan Wang, Runwen Zhu, Jianbo Zhao, Xiwu Chen, Siyu Zhang, Jiahao Gong, Qibin Zhou, Wenyuan Zhang, Ningzi Wang, Feiyang Tan, Hangning Zhou, Ziyao Xu, Haotian Yao, Chi Zhang, Xiaojun Liu, Xiaoguang Di, and Bin Li. Sparsead: Sparse query-centric paradigm for efficient end-to-end autonomous driving, 2024.
- [11] Mingzhe Guo, Zhipeng Zhang, Yuan He, Ke Wang, and Liping Jing. End-to-end autonomous driving without costly modularization and 3d manual annotation, 2024.
- [12] Haibao Yu, Wenxian Yang, Jiaru Zhong, Zhenwei Yang, Siqi Fan, Ping Luo, and Zaiqing Nie. End-to-end autonomous driving through v2x cooperation, 2024.
- [13] Wenzhao Zheng, Ruiqi Song, Xianda Guo, Chenming Zhang, and Long Chen. Genad: Generative end-to-end autonomous driving, 2024.
- [14] J. Gerdes and Eric Rossetter. A unified approach to driver assistance systems based on artificial potential fields. *Journal of Dynamic Systems Measurement and Control*, 123, 09 2001.
- [15] Jianqiang Wang, Jian Wu, Yang Li, and Keqiang Li. The concept and modeling of driving safety field based on driver-vehicle-road interactions. In *17th International IEEE Conference on Intelligent Transportation Systems (ITSC)*, pages 974–981, 2014.
- [16] Jianqiang Wang, Jian Wu, and Yang Li. The driving safety field based on driver-vehicle-road interactions. *IEEE Transactions on Intelligent Transportation Systems*, 16(4):2203–2214, 2015.
- [17] Jiayi Han, Jian Zhao, Bing Zhu, and Dongjian Song. Spatial-temporal risk field for intelligent connected vehicle in dynamic traffic and application in trajectory planning. *IEEE Transactions on Intelligent Transportation Systems*, 24(3):2963–2975, 2023.
- [18] Ye Tian, Huaxin Pei, Jingxuan Yang, Jianming Hu, Yi Zhang, and Xin Pei. An improved model of driving risk field for connected and automated vehicles. In *2021 IEEE International Intelligent Transportation Systems Conference (ITSC)*, Sep 2021.
- [19] Peter Hart, Nils Nilsson, and Bertram Raphael. A formal basis for the heuristic determination of minimum cost paths. *IEEE Transactions on Systems Science and Cybernetics*, page 100–107, 1968.
- [20] Ye Tian, Huaxin Pei, and Yi Zhang. Path planning for cavs considering dynamic obstacle avoidance based on improved driving risk field and a* algorithm. In *2020 5th International Conference on Information Science, Computer Technology and Transportation (ISCTT)*, Nov 2020.
- [21] Zhaojie Wang, Guangquan Lu, Haitian Tan, and Miaomiao Liu. A risk-field based motion planning method for multi-vehicle conflict scenario. *IEEE Transactions on Vehicular Technology*, PP:1–13, 01 2023.
- [22] Cheng Teng, Ligang Guo, Wu Zexu, Shi Qin, and Ni Hao. Car following model based on driving risk field for vehicle infrastructure cooperation. *2022 6th CAA International Conference on Vehicular Control and Intelligence (CVCI)*, pages 1–6, 2022.
- [23] Linheng Li, Jing Gan, Xinkai Ji, Xu Qu, and Bin Ran. Dynamic driving risk potential field model under the connected and automated vehicles environment and its application in car-following modeling. *IEEE Transactions on Intelligent Transportation Systems*, page 122–141, Jan 2022.
- [24] Ning Sun, Min Hu, Zeyang Zhang, Hang Du, and Shengxuan Zhao. Extension and application of driving risk field model considering vehicle motion constraints. *IEEE Access*, 11:109953–109963, 2023.
- [25] Yadollah Rasekhipour, Amir Khajepour, Shih-Ken Chen, and Bakhtiar Litkouhi. A potential field-based model predictive path-planning controller for autonomous road vehicles. *IEEE Transactions on Intelligent Transportation Systems*, page 1255–1267, May 2017.
- [26] Haitian Tan, Guangquan Lu, and Miaomiao Liu. Risk field model of driving and its application in modeling car-following behavior. *IEEE Transactions on Intelligent Transportation Systems*, page 11605–11620, Aug 2022.
- [27] Zhengcai Yang, Yunzhong Hu, and Youbing Zhang. Path-planning strategy for lane changing based on adaptive-grid risk-fields of autonomous vehicles. *World Electric Vehicle Journal*, 13(10), 2022.
- [28] Yuchun Wang, Boyang Wang, Xu Wang, Yingqi Tan, Jianyong Qi, and Jianwei Gong. A fusion of dynamic occupancy grid mapping and multi-object tracking based on lidar and camera sensors. In *2020 3rd International Conference on Unmanned Systems (ICUS)*, pages 107–112, 2020.
- [29] Zhao Liang, Shi Weiguang, Zhou Shenghao, and Chen Junwei. Research on occupancy grid map creation method based on rpb-fusion. In *2023 8th Asia-Pacific Conference on Intelligent Robot Systems (ACIRS)*, pages 80–83, 2023.
- [30] Hao Li, Manabu Tsukada, Fawzi Nashashibi, and Michel Parent. Multi-vehicle cooperative local mapping: A methodology based on occupancy grid map merging. *IEEE Transactions on Intelligent Transportation Systems*, 15(5):2089–2100, 2014.
- [31] Yuichiro Toda and Naoyuki Kubota. Path planning using multi-resolution map for a mobile robot. In *SICE Annual Conference 2011*, pages 1276–1281, 2011.
- [32] Çağan Önen, Ashish Pandharipande, Geethu Joseph, and Nitin Jonathan Myers. Occupancy grid mapping for automotive driving exploring clustered sparsity. *IEEE Sensors Journal*, 24(7):9240–9250, 2024.
- [33] Simone Mentasti and Matteo Matteucci. Multi-layer occupancy grid mapping for autonomous vehicles navigation. In *2019 AEIT International Conference of Electrical and Electronic Technologies for Automotive (AEIT AUTOMOTIVE)*, pages 1–6, 2019.
- [34] Jakub Porebski, Krzysztof Kogut, Paweł Markiewicz, and Paweł Skruc. Occupancy grid for static environment perception in series automotive applications. *IFAC-PapersOnLine*, 52(8):148–153, 2019. 10th IFAC Symposium on Intelligent Autonomous Vehicles IAV 2019.
- [35] Yi Jin, Marcel Hoffmann, Anastasios Deligiannis, Juan-Carlos Fuentes-Michel, and Martin Vossiek. Semantic segmentation-based occupancy grid map learning with automotive radar raw data. *IEEE Transactions on Intelligent Vehicles*, 9(1):216–230, 2024.
- [36] Xinhua Zheng, Yuru Li, Dongliang Duan, Liuqing Yang, Chen Chen, and Xiang Cheng. Multivehicle multisensor occupancy grid maps (mvms-ogm) for autonomous driving. *IEEE Internet of Things Journal*, 9:22944–22957, 2022.
- [37] Steven M. LaValle. Rapidly-exploring random trees: a new tool for path planning. *The annual research report, The annual research report*, Jan 1998.
- [38] Sertac Karaman and Emilio Frazzoli. Optimal kinodynamic motion planning using incremental sampling-based methods. In *49th IEEE Conference on Decision and Control (CDC)*, Dec 2010.
- [39] P. Pharpatara, B. Herisse, and Y. Bestaoui. 3-d trajectory planning of aerial vehicles using rrt*. *IEEE Transactions on Control Systems Technology*, 25(3):1116–1123, May 2017.
- [40] Zezhong Wang and Chongfeng Wei. Human-centred risk-potential-based trajectory planning of autonomous vehicles. *Proceedings of the Institution of Mechanical Engineers, Part D: Journal of Automobile Engineering*, 237(2–3):393–409, Feb 2023.
- [41] Haibao Yu, Yizhen Luo, Mao Shu, Yiyi Huo, Zebang Yang, Yifeng Shi, Zhonglong Guo, Hanyu Li, Xing Hu, Jirui Yuan, and Zaiqing Nie. Dair-v2x: A large-scale dataset for vehicle-infrastructure cooperative 3d object detection. *2022 IEEE/CVF Conference on Computer Vision and Pattern Recognition (CVPR)*, pages 21329–21338, 2022.
- [42] Moritz Werling, Julius Ziegler, Sören Kammel, and Sebastian Thrun. Optimal trajectory generation for dynamic street scenarios in a frenet frame. In *2010 IEEE International Conference on Robotics and Automation*, pages 987–993, 2010.



Jiaxing Chen received an M.S. degree in Electrical and Computer Engineering from the University of Illinois, Chicago, USA, in 2021 and worked as an Algorithm engineer at the National Innovation Center of Intelligent and Connected Vehicles, Beijing, China from 2021 to 2022. He is currently pursuing a Ph.D. degree at the School of Vehicle and Mobility, Tsinghua University, Beijing, China. Chen’s research interests include computer vision and perception based on Vehicle-Road-Cloud architecture.



Jiayi Liu received the B.E. and M.E. degrees in Mechanical Engineering at the School of Vehicle and Mobility, Tsinghua University. He is now pursuing a Ph.D. degree in civil engineering at the University of Wisconsin-Madison. His research interests include collaborative perception, real-time perception, Vehicle-Road-Cloud integration systems, and cyber-physical system architecture design.



Wei Zhong received the B.S. degree and Ph.D. from Tsinghua University in 2010 and 2016, respectively. In 2013, she went to the University of Michigan (Ann Arbor) for a research visit at the Department of Mechanical Engineering. From 2019 to 2021, she conducted postdoctoral research at Tsinghua University. She is currently an Assistant Researcher at the State Key Laboratory of Intelligent Green Vehicle and Mobility at Tsinghua University. Her research interests mainly focus on intelligent connected vehicles, including system architecture, multi-objective

optimization, and cloud control platforms.



Yanbo Lu received the B.S. degree in Mechanical engineering from Nanjing University of Aeronautics and Astronautics, China in 2017, the M.S degree in Mechanical engineering from Embry-Riddle Aeronautical University, USA in 2018, and the Ph.D degree in Mechanical Engineering from Southeast University, China in 2023. He is currently a Post-Doctoral Research Fellow with the School of Vehicle and Mobility, Tsinghua University. His research interests include vehicle dynamics and control, vehicle-cloud control system and fault-tolerant

control.



Bolin Gao received the B.E. and M.E. degrees in Vehicle Engineering from Jilin University, Changchun, China, in 2007 and 2009, respectively, and the Ph.D. degree in Vehicle Engineering from Tongji University, Shanghai, China, in 2013. He is now an associate research professor at the School of Vehicle and Mobility, Tsinghua University. His research interests include the theoretical research and engineering application of the dynamic design and control of Intelligent and Connected Vehicles, especially collaborative perception and tracking methods

in cloud control systems, intelligent predictive cruise control systems on commercial trucks with cloud control mode, as well as the test and evaluation of intelligent vehicle driving system.



Jin Huang received the B.E. and Ph.D. degrees from the College of Mechanical and Vehicle Engineering, Hunan University, Changsha, China, in 2012 and 2006, respectively. From 2009 to 2011, he was also a joint Ph.D. with the George W. Woodruff School of Mechanical Engineering, Georgia Institute of Technology, Atlanta, GA, USA. He started his career as a Postdoc and an Assistant Research Professor at Tsinghua University, Beijing, China, in 2013 and 2016, respectively. His research interests include artificial intelligence in intelligent transportation systems, dynamics control, and fuzzy engineering.

tems, dynamics control, and fuzzy engineering.



Yifei Liu received his bachelor’s and master’s degrees from Huazhong University of Science and Technology in China in 2020 and the University of Bristol in the United Kingdom in 2023. He is currently working as an engineer in the Intelligent Connected Vehicle Research Group at the School of Vehicle and Mobility at Tsinghua University. His main research direction is road section perception and fusion under the Vehicle-Road-Cloud integrated architecture.



Hengduo Zou is pursuing a B.E. degree in Mechanical Engineering at the School of Vehicle and Mobility, Tsinghua University. His research interests include autonomous driving, computer vision, and Vehicle-Road-Cloud integration systems.



Zhihua Zhong received a Ph.D. degree in engineering from Linkoping University, Linkoping, Sweden, in 1988. He is currently a Professor at the School of Vehicle and Mobility, Tsinghua University, Beijing, China. He was elected Member of the Chinese Academy of Engineering in 2005. His research interests include auto collision security technology, the punching and shaping technologies of the auto body, modularity and light-weighting auto technologies, and vehicle dynamics.